Pergamon

Geochimica et Cosmochimica Acta, Vol. 68, No. 12, pp. 2693–2698, 2004

0016-7037/04 $30.00 + .00

doi:10.1016/j.gca.2003.12.006

# Interdiffusion of $H_2O$ and $CO_2$ in metamorphic fluids at ~490 to 690°C and 1 GPa

DAVID A. WARK* and E. BRUCE WATSON

Department of Earth and Environmental Sciences, Rensselaer Polytechnic Institute, Troy, NY 12180, USA

(*Received August* 12, 2002; *accepted in revised form December* 8, 2003)

**Abstract**—Interdiffusion coefficients have been determined for $H_2O$-$CO_2$ mixtures by quantifying the flux of $CO_2$ between two fluid-filled chambers in a specially designed piston-cylinder cell. The two chambers, which are maintained at 1.0 GPa and at temperatures differing by ~100°C, each contain the $X_{CO2}$-buffering assemblage calcite + quartz + wollastonite, in $H_2O$. The positive dependence of $X_{CO2}$ on temperature results in a down-temperature, steady-state flux of $CO_2$ through a capillary tube that connects the two chambers. This flux drives the wollastonite = calcite + quartz equilibrium to the right in the cooler chamber, producing a measurable amount of calcite that is directly related to $CO_2$-$H_2O$ interdiffusion rates. Diffusivities calculated from seven experiments range from $1.0 \times 10^{-8}$ to $6.1 \times 10^{-8}$ $m^2/s$ for mean capillary temperatures between ~490 and 690°C. The data set can be approximated by an Arrhenius-type relation:

$$D = 4.7 \times 10^{-6} \exp(-4560/T)\ m^2/s$$

($T$ in K), which yields values within a factor of 2 of, but slightly lower than, diffusivities estimated by application of the Stokes-Einstein relation.

Because rates of $H_2O$ and $CO_2$ interdiffusion approach (within 1 to 2 orders of magnitude) rates of heat conduction in rocks, rapid $CO_2$-$H_2O$ interdiffusion should be expected in deep-seated fluids wherever gradients in $X_{CO2}$ are imposed by contrasting mineral assemblages. Considering the small-scale heterogeneity of the crust, strong gradients in $X_{CO2}$ are probably quite common, particularly where different carbonate-bearing assemblages are juxtaposed or where they are interlayered with carbonate-absent rocks. Cross-layer, diffusive mass transfer of $CO_2$ and $H_2O$ may play an important role in driving dehydration and decarbonation reactions, even in the absence of fluid flow. 

## 1. INTRODUCTION

Carbon dioxide and water are the main components of volatile species in Earth's upper mantle and crust. Because of their high mobility and their ability to dissolve mineral components, deep-seated $CO_2$ and $H_2O$ fluids play a critical role in the geochemical evolution of our planet where they reside at depth (e.g., Walther and Orville, 1982; Etheridge et al., 1984) and (after they have escaped) in the atmosphere and hydrosphere (e.g., Berner et al., 1983; Kerrick and Caldeira, 1998). In recognition of their geochemical importance, much work has been done to characterize the thermodynamic properties of mixed $CO_2$-$H_2O$ fluids (e.g., Greenwood, 1973; Kerrick and Jacobs, 1981; Aranovich and Newton, 1999; Blencoe et al., 1999; Seitz and Blencoe, 1999), and to understand how the composition of such fluids influences their transport through rocks (e.g., Watson and Brenan, 1987; Holness, 1992).

Increasingly, non-equilibrium processes, such as the interdiffusion of $H_2O$ and $CO_2$ due to spatial variation in fluid composition, are recognized as also having played important roles in the evolution of many deep-seated fluid-rock systems. Although it has long been recognized that interdiffusion can affect the metamorphic history of some rocks on a small (i.e., centimeter) scale (e.g., Hewitt, 1973; Labotka et al., 1988; Ague and Rye, 1999; Ague, 2000, 2002), many petrologists have considered diffusion relatively unimportant at the large spatial scale (hundreds of meters) of most metamorphic systems. Recently, however, some workers (Skelton et al., 1997; Lasaga et al., 2001) have argued that $H_2O$-$CO_2$ interdiffusion can play an important role in such systems, on time-scales of $10^5$ to $10^7$ years.

Until now, most efforts to model the consequences of $H_2O$ and $CO_2$ interdiffusion in natural systems have relied upon interdiffusion rates measured for mixtures of $H_2O$ and $CO_2$ at atmospheric pressures (e.g., Frank et al., 1996), or calculated for other (similar) species using estimated viscosities of water combined with the Stokes-Einstein equation (e.g., Walton, 1960), or using the Nernst-Einstein equation with electrical conductance in solutions of water and various ions (Oelkers and Helgeson, 1988). To our knowledge, no direct measurements of $H_2O$-$CO_2$ interdiffusion have been made at the temperatures and pressures of interest to those modeling processes in the mantle or the deep crust. Such measurements are warranted not only to assess the validity of values extrapolated from 1-atm data, but also because of the possibility that diffusion coefficients will be affected by presence of other components (e.g., silica) in natural, deep-seated fluids.

In this paper we present results of experiments designed to quantify the rates of $H_2O$-$CO_2$ interdiffusion in a fluid equilibrated with a common metamorphic assemblage, at conditions like those in the deep crust. The experiments were conducted by connecting two reservoirs, each at a different temperature ($T$) and each containing the assemblage calcite + quartz + wollastonite + $H_2O$, with a capillary tube. Because this assemblage is a $T$-sensitive buffer of $X_{CO2}$, gradients in fluid composition (and hence, chemical potential) were established, leading to interdiffusion of $H_2O$ and $CO_2$. By monitoring reaction

* Author to whom correspondence should be addressed (warkd@rpi.edu).

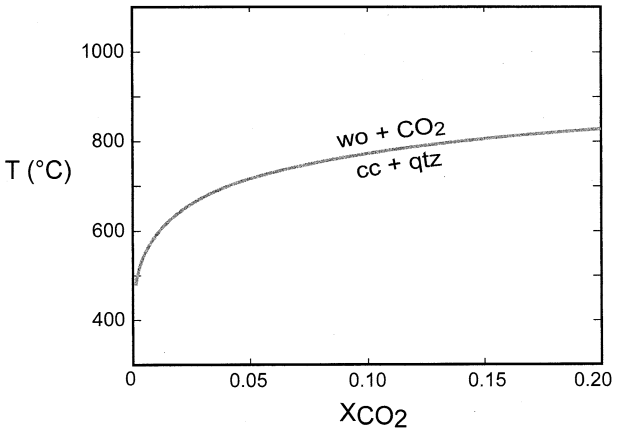


Fig. 1. *T* vs. $X_{CO2}$ for reaction 1 at 1.0 GPa, calculated using the program Thermocalc (Powell and Holland, 1988).

progress, we were able to estimate the amount of $CO_2$ transported, from which we calculated diffusion coefficients.

## 2. EXPERIMENTS

### 2.1. DSD Cell Design

Characterization of diffusion coefficients in silicate melts is relatively straightforward because concentration gradients can be preserved for analysis by quenching. This approach cannot be applied, however, to determine diffusivities in supercritical, C-O-H fluids at deep crustal or mantle conditions. To overcome this complication, Watson and Wark (1997) designed a pressure-sealing, "differential solubility and diffusion," or DSD cell, to characterize the diffusivity of silica (as $H_4SiO_4$ polymers) in supercritical $H_2O$. This cell design was adopted to take advantage of the temperature dependence of silica solubility: by imposing different temperatures on two "chambers" containing quartz and $H_2O$, a gradient in the concentration of dissolved silica was established in a fluid-filled capillary that connected the two. The temperature difference was achieved by positioning one end of the DSD near the midpoint of a graphite-furnace, piston-cylinder apparatus, where the temperature was hottest. Because temperature drops off toward either end of the furnace, the opposite end of the DSD was cooler, resulting in a lower concentration of dissolved $SiO_2$. The consequent gradient in chemical potential resulted in diffusive transport of silica through the capillary toward the cooler end of the DSD cell. By measuring the amount of silica precipitated there, Watson and Wark (1997) were able to estimate diffusion coefficients for a range of temperatures.

We initially attempted to apply the same experimental design used by Watson and Wark (1997) in this study of $CO_2$-$H_2O$ interdiffusion, reasoning that we could establish a gradient in $X_{CO2}$ by subjecting all phases in the well-known, univariant decarbonation reaction

$$\text{calcite} + \text{quartz} = \text{wollastonite} + CO_2 \qquad (1)$$

to different temperatures at each end of a water-filled DSD cell, because for a given *P*, $X_{CO2}$ will vary with *T* (Fig. 1) if all phases are present.

With the goal of preventing newly-precipitated calcite from falling down the capillary tube, experiments were performed with the DSD cell situated *below* the furnace hot spot, and with wollastonite in the lower (cooler) chamber and calcite plus quartz in the upper (hotter) chamber. In these experiments, calcite and quartz react to form wollastonite and to produce $CO_2$. As $X_{CO2}$ of the fluid increases from its starting value near zero to the value defined by the univariant reaction curve for the temperature of the hottest point in the chamber, $CO_2$ diffuses down the concentration (chemical potential) gradient toward the cooler chamber. Consequently, $X_{CO2}$ in the cooler chamber rises until it intersects the reaction boundary for the temperature of that chamber, at which point wollastonite begins to react to calcite plus quartz. From this point on, $X_{CO2}$ is buffered at a near-constant value in each chamber as long as all three solid phases remain, resulting in steady-state exchange (via interdiffusion) of $H_2O$ and $CO_2$.

The main drawback of performing experiments centered below the hot spot is that only a limited volume of calcite and quartz can be added to the upper (hotter) chamber before we risk having either phase fall into the capillary tube. On the other hand, by adding smaller quantities of these phases we risk the possibility that one or both will be depleted as they go into solution and as $CO_2$ diffuses through the capillary to the cooler DSD cell. With the goal of circumventing these problems, we made minor changes to the original DSD design. First, we raised the height of the capillary tube, allowing us to increase the relative amount of reactants (calcite + quartz) added to the upper chamber. The added height of the capillary tube, however, increased the likelihood that its top would contact, and seal against, the chamber's "roof" during the minor compaction that accompanies pressurization to run conditions. We were able to reduce the likelihood of this happening by adding a "washer" to the top of the DSD assembly, which forced most compaction to take place along the capsule margins.

The resulting experimental assembly (Fig. 2) consisted of a DSD cell containing two chambers connected by a piece of platinum tubing ~1 cm in length, and 0.04 or 0.08 cm inner diameter. A Mo sleeve surrounded the central portion of the cell to prevent deformation of the capillary tube; the Mo, and the top and bottom portions of the DSD cell, were surrounded by sleeves of silica or Pyrex glass (for high and low temperature runs, respectively). Capping the cell was a silver lid. Cylinders of molybdenum with sleeves of silica glass were positioned above and below the DSD cell to flatten the temperature gradients. Finally, crushable MgO pieces were added to fill the remaining volume of the graphite furnace (not shown), which was then surrounded by Pyrex, NaCl, and Pb foil sleeves.

To characterize the temperature gradient, thermocouples—each capable of measuring temperature in two places—were positioned above and below the assembly (Fig. 3). The thermocouples rested within wells in the molybdenum cylinders at each end of the DSD cell. For details on the characterization of temperature profiles and other aspects of DSD cell design, the reader is referred to Watson and Wark (1997).

### 2.2. Starting Materials

Starting materials included natural crystals of wollastonite, quartz, and calcite. The wollastonite, from Willsboro, New York, was ground to splinters typically <2 mm in length, hand picked under an optical microscope to remove pieces containing clinopyroxene or garnet, then rinsed in dilute HCl. Calcite ("Iceland spar" from Mexico), and quartz (optically clear and inclusion-free crystals from Arkansas) were ground in agate and sieved to size fractions of ~50 to 150 $\mu$m. After grinding and sieving, all starting minerals were rinsed in distilled $H_2O$ to remove fine particles that tended to float.

### 2.3. Conducting a DSD Experiment

Before an experiment, we packed enough wollastonite into the lower chamber so that it would be almost full when the two capsule pieces were assembled. We then determined the amount of distilled water that would fill the void space in the same chamber after the two pieces were joined. After adding more water to the lower chamber, we pressed the two pieces together, which resulted in transport of the excess $H_2O$ upward through the capillary. Over the next several minutes, the assembly was checked for leaks by visual inspection of both the height of the water in the capillary tube and of the seam where the two capsule pieces were joined.

Next, the upper chamber of the DSD cell was loaded with a calcite + quartz mixture, leaving 1 to 2 mm to the top of the platinum capillary tube. We then added (and weighed) distilled water to the rim. After adding the remaining parts of the assembly, it was pressurized to 1.0 GPa in the piston cylinder. Next, the temperature was ramped up to the desired value for one of the four thermocouple positions. Temperatures for each of these positions were monitored throughout the duration of an experiment. Average values were then interpolated to estimate temperatures in the chambers of the cells where the $CO_2$-buffering reactions were taking place (Fig. 3).

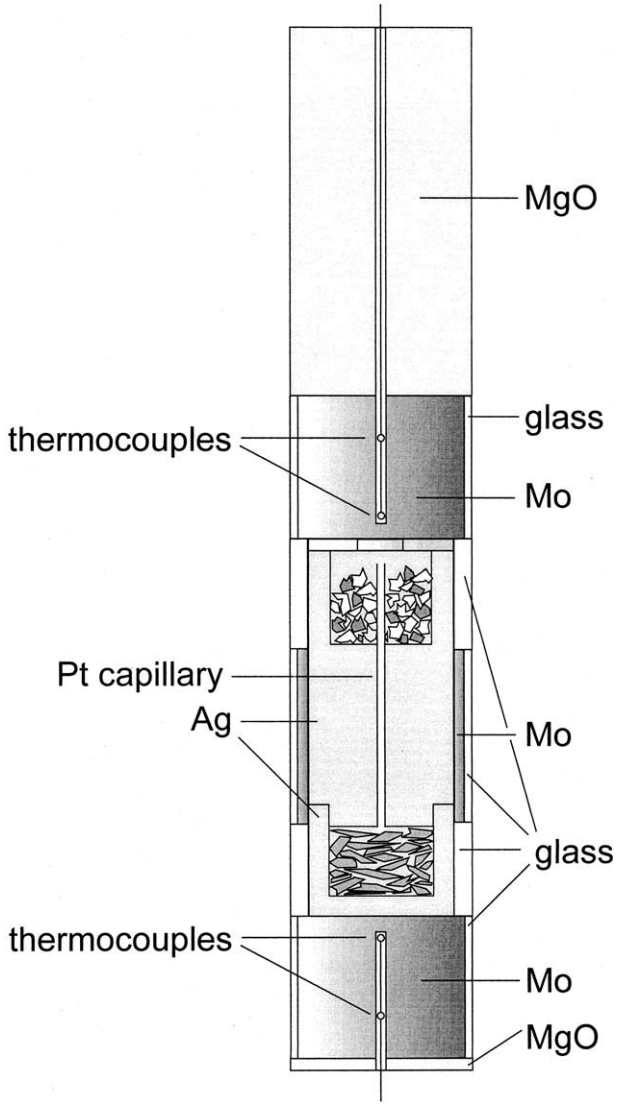


Fig. 2. DSD cell, centered below the furnace hot spot, employed in this study with representative temperature profile. Calcite and quartz are shown in upper (hotter) chamber, wollastonite in lower (cooler) chamber. See text for details.

At the termination of an experiment, the capsule was frozen in liquid nitrogen to immobilize the contents and to embrittle the molybdenum sleeve. This sleeve was broken with a hammer and removed, after which the silver capsule was cut with pruning shears midway along its axis. This isolated the two chambers and their contents, which were captured, and allowed to dry in, separate Teflon jars. With the goal of measuring the $CO_2$ sequestered in calcite, and to confirm that the capillary did not contact and seal against the top of the upper chamber, we exposed its contents by peeling away the lid. To expose the contents of the lower chamber, we severed it with pruning shears.

The final step involved measurement of the $CO_2$ contained within calcite in each chamber. This was accomplished by measuring the amount of gas expelled after immersing each chamber and its contents in HCl within a glass extraction vessel (Fig. 4) attached to a mercury manometer. The manometer was calibrated by applying the same technique to known amounts of calcite. The amount of $CO_2$ transported to the colder reservoir was then calculated as that contained within calcite, combined with the amount in solution at run conditions, which was calculated using version 2.5 of program Thermocalc (Powell and Holland, 1988).

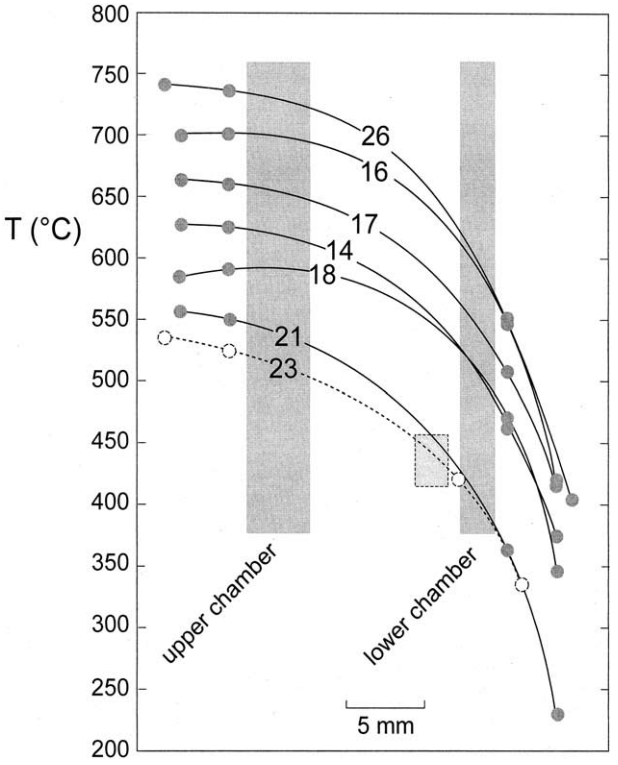


Fig. 3. Measured temperatures (circles) and interpolated profiles for each of the four experiments reported in this study.

### 2.4. Extracting Diffusion Coefficients

A diffusion coefficient, $D$, was determined for each experiment by applying Fick's first law:

$$J = \frac{m}{At} = -D\frac{\Delta C}{\Delta z}, \tag{2}$$

knowing the length ($\Delta z$) of the capillary, the difference in $CO_2$ concentration between the two chambers ($\Delta C$), and the flux ($J$), which was determined from the total amount of $CO_2$ ($m$) that was transported across the capillary cross section ($A$) in a given time ($t$). Of course, there must be a range of $D$ values applicable to any one experiment, because temperature varies along the length of the capillary through which $H_2O$ and $CO_2$ diffuse. As a consequence, one might expect diffusive transport to be rate-limited at the coolest end of the capillary, such that the calculated $D$ value would correspond with the temperature

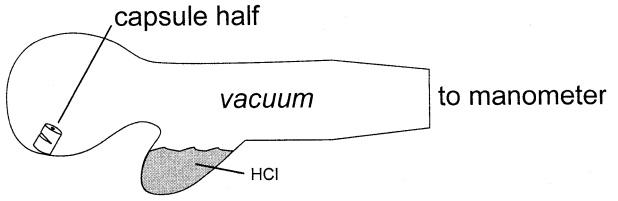


Fig. 4. Glass reaction tube, which was attached to mercury manometer, for measurement of $CO_2$ contained in calcite of each chamber after completion of diffusion experiment. Portion of capsule (either upper or lower half) was inserted in far end of reaction tube, after which HCl was added to lower reservoir. After pumping to zero reading on manometer ($\sim 10^{-4}$ torr) using rotary vacuum pump, the system was sealed by closing all valves. The reaction tube was then tilted upright so that the capsule was immersed in acid, thereby releasing $CO_2$.

there. This, however, isn't the case: because the steady-state flux of diffusing components, $J$, must be uniform throughout the length of the capillary, the local concentration gradient, $dC/dz$, must steepen to compensate for the decrease in $D$ values toward the cooler end. Numerical modeling shows that this leads to a "bowing" upward of the concentration profile (see Fig. 5A of Watson and Wark, 1997), such that the *local* concentration gradient ($dC/dz$) at the high-temperature end is shallower than the overall gradient ($\Delta C/\Delta z$) between the two DSD cells, whereas $dC/dz$ is steeper at the cooler end. At the position of the mean temperature in the capillary, $dC/dz = \Delta C/\Delta z$, and the $D$ value calculated using Eqn. 2 applies. We refer to this as the "effective" temperature, which we estimate using $T_{eff} = T_{low} + 0.62 \times (T_{high} - T_{low})$ (see Watson and Wark, 1997).

An important assumption in our investigation is that steady-state transport of $CO_2$ and $H_2O$ is rate-limited by diffusion and not by the rate at which reaction 1 proceeds. We assessed this in part by applying a finite-difference computer code (see Watson and Wark, 1997) to simulate interdiffusion of $CO_2$ and $H_2O$ in the DSD cell. A critical variable in that code is the mass transfer coefficient, $k$, which gives the number of moles of $CO_2$ produced, per square centimeter of exposed reactant surface area, per second. For simulations assuming sufficiently high $k$, the amount of $CO_2$ produced by reaction will satisfy the diffusive flux. Assuming that the appropriate $k$ values for $CO_2$ production by reaction 1 (which are not known) are similar to values applicable to quartz dissolution ($1 \times 10^{-7}$; Tester et al., 1994), our simulations show that steady-state $CO_2$ transport is diffusion controlled. For $k$ values $<\sim 1 \times 10^{-8}$ mol/cm$^2$-s, however, $CO_2$ would not be produced rapidly enough, and its rate of transport through the capillary would be controlled by the rate of reaction.

Evidence that the mass transfer coefficient is above $1 \times 10^{-8}$ mole/cm$^2$-s, and hence that the rate of $CO_2$ transport through the capillary is controlled by diffusion and not by reaction, comes from results of an earlier study that focused on changes in the geometry of fluid-filled pores in a temperature gradient (Wark and Watson, 2002). Some of the experiments in that study were conducted with $P$ and $T$ conditions and with relative amounts of calcite and quartz like those in our $CO_2$-$H_2O$ interdiffusion experiments. Reaction rates were much faster, however: in only four hours, at least 75% of available calcite had reacted with quartz to form wollastonite at the hotter end of the capsules. In all of the interdiffusion experiments, by contrast, no more than ~5% of the starting calcite reacted in the same amount of time. This difference can be attributed to the absence of a capillary tube (or a similar restriction) and the greater amount of fluid (which formed interconnected pores) in the pore geometry experiments, which allowed reaction 1 to proceed at a rate dictated by reaction kinetics, and not by the rate of $CO_2$ transport away from the reaction site.

Another important assumption is that reaction 1 takes place fast enough, and that diffusive transport is rapid enough, that the time required for $X_{CO2}$ to reach equilibrium levels in each chamber is short relative to the total time of an experiment. If so, steady-state transport could be assumed for the entire duration of the experiment for the purposes of calculating diffusivities. The same finite-difference computer code was used to assess this assumption: as concluded by Watson and Wark (1997) for their study of silica diffusion in supercritical $H_2O$, our simulations confirmed that the time required to reach steady state was only a small fraction of run duration, and was thus inconsequential to the diffusivity calculation.

### 2.5. Estimating Errors

Uncertainties in calculated diffusion coefficients have multiple contributions. The smallest errors were associated with measurement of the length and diameter of the capillary (each contributing 5%). A much larger contribution (~25%) arose from the range of possible temperatures in each chamber of the DSD cell. For each experiment, this contribution was based on the highest and lowest $X_{CO2}$ values (from which we estimated the highest and lowest $X_{CO2}$ gradients) allowed by interpolation between temperatures measured at the four thermocouple positions.

The final source of error is the uncertainty in measuring $CO_2$ in run products by manometry. Ideally, the starting mass of calcite would match that required to generate the $CO_2$ calculated to be in solution during the run, plus the mass of calcite measured in each chamber after the experiment is terminated. In some experiments, the amount measured by manometry, when combined with the amount calculated to be in solution, was higher than the starting amount (in the worst case, 15% higher for experiments #17 and #18). In others, the amount measured was relatively low (at worst, ~6% low for # 21 and #23). Where there appeared to be "excess" $CO_2$ (i.e., the measured amount was high) we subtracted this "excess" from the amount measured in the cooler chamber to provide a minimum value for $m$ in Eqn. 2; where too little $CO_2$ was measured, we added the deficit to the amount measured in the lower chamber, providing an upper bound to $m$.

## 3. RESULTS

Table 1 summarizes run conditions and calculated diffusivities for seven successful experiments. Not reported are a multitude of experiments for which one or more thermocouples failed (thereby preventing accurate estimate of $X_{CO2}$ in either chamber) and those for which the capillary tube became plugged by contact with the lid to the DSD assembly. Reported errors for $D$ reflect the uncertainties described above.

Effective temperatures for successful experiments span only ~200°C due to experimental limitations at temperatures outside of the investigated range. The highest temperature at which experiments could be conducted was limited by the amount of calcite plus quartz that we could load into the hotter chamber: at mean temperatures > 700°C or so, the equilibrium $X_{CO2}$ value was so high in the upper chamber that the reactants were consumed before steady-state transport of $CO_2$ and $H_2O$ could be achieved. At low temperatures (<450°C), we were limited primarily by the shallowing of concentration gradients, and hence by the long duration needed to conduct an experiment.

As shown in Figure 5, the seven values reported, which vary by over half an order of magnitude (from $1.0 \times 10^{-8}$ to $6.1 \times$

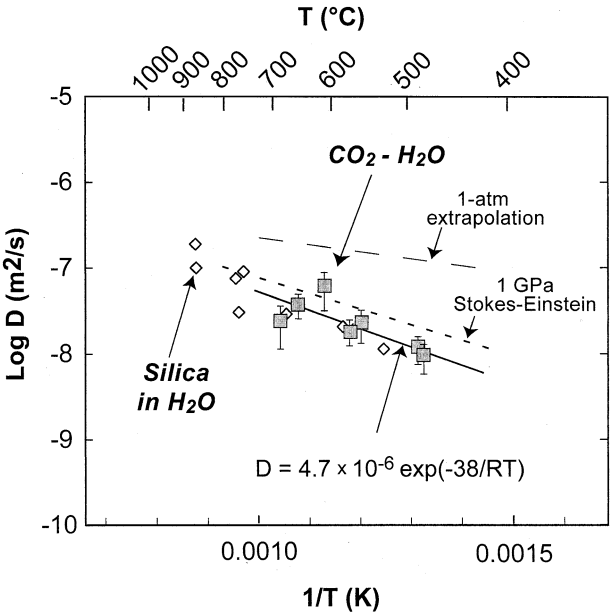


Fig. 5. Plot of log $D$ vs. $1/T$. Measured $CO_2$-$H_2O$ interdiffusion coefficients, with error bars, are shown as squares; thick, solid line, shows linear regression to the $CO_2$-$H_2O$ data. Calculated $CO_2$ diffusivities, using the Stokes-Einstein equation, are shown by lower dashed line. Upper dashed line shows diffusivities determined by extrapolation of low-$T$, 1-atm data of Frank et al. (1996). Measured values for silica diffusion in $H_2O$ (diamonds) from Watson and Wark (1997).

Table 1. Summary of experimental conditions and results.

| Number | Duration (h) | $T_h$ (°C) | $T_c$ (°C) | $T_{eff}$[a] (°C) | ΔC (mol/cm$^3$) | Capillary length (cm) | Capillary diameter (cm) | $CO_2$ transported (moles × $10^5$)# | $D$[b] (m$^2$/s × $10^8$) |
|---|---|---|---|---|---|---|---|---|---|
| DCO2-14 | 120 | 618 | 508 | 576 | 0.00045 | 0.9 | 0.04 | 5.0 | 1.9 ± 0.7 |
| DCO2-16 | 48 | 697 | 589 | 656 | 0.00125 | 1.0 | 0.04 | 10 | 3.7 ± 1.3 |
| DCO2-17 | 72 | 653 | 549 | 613 | 0.00094 | 1.0 | 0.04 | 14 | 6.1 ± 3.4 |
| DCO2-18 | 240 | 592 | 509 | 560 | 0.00027 | 1.0 | 0.04 | 6.5 | 2.2 ± 1.1 |
| DCO2-21 | 480 | 539 | 408 | 489 | 0.00014 | 1.0 | 0.08 | 14 | 1.2 ± 0.4 |
| DCO2-23 | 401 | 512 | 443 | 486 | 0.00007 | 0.65 | 0.08 | 7.8 | 1.0 ± 0.5 |
| DCO2-26 | 36 | 728 | 624 | 688 | 0.00172 | 0.88 | 0.04 | 7.7 | 2.4 ± 1.5 |

[a] $T_{eff} = T_c + .62 \times (T_b - T_c)$, based on Watson and Wark (1997).
[b] Includes amount needed to saturate cooler cell.

$10^{-8}$ m$^2$/s), increase with temperature despite strong scatter at the high temperature end. A weighted linear regression through the data points (solid line) can be described by the Arrhenius relation:

$$D = 4.7(\pm 0.6) \times 10^{-6} \exp[-4560(\pm 1440)/T] \text{ m}^2/\text{s}, \quad (3)$$

where $T$ is in kelvins. Interestingly, the $CO_2$-$H_2O$ data overlap the diffusivity values of Watson and Wark (1997) for diffusion of $SiO_2$ in supercritical $H_2O$ (diamonds), although the activation energy for $SiO_2$ is slightly higher (52 kJ/mol). This overlap is not altogether surprising, considering that the $CO_2$ molecule and a $H_4SiO_4$ polymer are likely to be similar in size. Still, the $CO_2$ molecule is probably smaller, based on the smaller size of the carbon atom relative to silicon (by ~2/3), and on the fact that the $Si(OH)_4$ tetrahedron can be considered roughly equidimensional, in contrast with the rod-like shape (and hence smaller *average* radius) of the $CO_2$ molecule.

We can compare the measured values for $CO_2$-$H_2O$ interdiffusion with those determined by applying the Stokes-Einstein relation, which assumes that a molecule diffusing through a liquid can be modeled as a sphere traveling through a viscous medium:

$$D = \frac{k_B T}{6\pi\eta R_0}, \quad (4)$$

where $D$ is the diffusivity for a particular temperature $T$, and $k_B$ is the Boltzmann constant, $\eta$ is the viscosity of the solvent, and $R_0$ is the radius of the diffusing molecule. Viscosities of supercritical $CO_2$-$H_2O$ fluids are not known at the conditions of our experiments, but they can be estimated using the method applied to supercritical $H_2O$ by Watson and Wark (1997). This method involves extrapolation from viscosity data available for lower $T$ and $P$, by applying a relation linking molar volume to viscosity of simple liquids (their Eqn. 4). Using that relation (and the same constants), but inserting molar volumes for $CO_2$-$H_2O$ liquids from Duan et al. (1996), we calculated viscosities for fluids like those in our study. These were used, in turn, to calculate $D$ values for $CO_2$ from Eqn. 4, assuming that the average radius of the $CO_2$ molecule is 0.145 nm, or half that of an $Si(OH)_4$ tetrahedron. This value is also close to (but 75% of) the radius of a $CO_2$ molecule based on the assumption that it is half the collision diameter in the gas (Cussler, 1997, p. 105).

On the Arrhenius diagram (Fig. 5) the calculated diffusivities (lower dashed line) are displaced to values higher than, but roughly within a factor of 2 of, most of the measured values. A linear regression to the portion of the curve between 400 and 800°C yields a simple Arrhenius-type relation:

$$D = 5 \times 10^{-6} \exp(-4170/T) \text{ m}^2/\text{s}, \quad (5)$$

(with $T$ in K) that predicts a 10-fold increase in diffusivity, from $1 \times 10^{-8}$ to $1 \times 10^{-7}$ m$^2$/s, over this 400°C temperature range. The calculated activation energy for this curve is 35 kJ/mol, which is virtually identical to the value of 38 kJ/mol that was determined by linear regression through our seven data points (Eqn. 3).

Figure 5 also includes (upper dashed line) the extrapolation of a 1-atm, low-temperature ($T$ <50 °C) Arrhenius relation for $CO_2$ in water from Frank et al. (1996). Not surprisingly, the extrapolated 1-atm values do not match those measured in our experiments (the extrapolated values are higher by a factor of 5–10 in the 500–700°C range), and the calculated, 1-atm activation energy is lower, at 17 kJ/mol. This simply highlights the risk of extrapolating 1-atm data to high $P$ and $T$ conditions, especially for a fluid, the physical properties of which can change dramatically above the critical point.

## 4. APPLICATION TO MODELING FLUID EVOLUTION IN DEEP-SEATED SYSTEMS

The Arrhenius relation that describes our measured $CO_2$-$H_2O$ interdiffusion coefficients (Eqn. 3) can be used to predict diffusivities appropriate to modeling the evolution of deep-seated fluid-rock systems. While most workers already recognize that $CO_2$-$H_2O$ interdiffusion rates are high (relative to values appropriate to minerals and glasses, at least) until now there has been limited agreement on appropriate $D$ values.

Three recent papers, for example, apply diffusivities that vary by up to an order of magnitude in studies of metamorphic systems at ~500°C. Ague and Rye (1999) used a value for $D$ of $1 \times 10^{-8}$ (based on the work of Nigrini, 1970) in their study of Acadian prograde metamorphism. In their modeling of Caledonian metamorphism in Scotland, Skelton et al. (1997) used a value only slightly higher ($1.7 \times 10^{-8}$ m$^2$/s) that they based on the diffusivity of oxygen calculated using the Stokes-Einstein relation. And finally, Lasaga et al. (2001) used a "typical value" of $1 \times 10^{-7}$ m$^2$/s in their application of a non-equilibrium model to predict fluid flow during regional metamorphism.

The first two values agree well with extrapolation of our data using Eqn. 3, which yields a diffusivity of $1.4 \times 10^{-8}$ m$^2$/s at 500°C. The $1 \times 10^{-7}$ value used by Lasaga et al. (2001), in contrast, appears much too high, and more relevant to temper-

atures closer to ~900°C. This, of course, does not invalidate the general approach of Lasaga et al. (2001) to calculating fluid fluxes, but the contribution to these fluxes by $CO_2$ diffusion may be less than is shown in their examples. Perhaps more importantly, however, a general conclusion reached by each of these authors still holds: fluids are likely to be compositionally heterogeneous in many metamorphic systems, and rapid $CO_2$-$H_2O$ interdiffusion can play an important role in driving dehydration and decarbonation reactions, with or without fluid flow. Effects of such interdiffusion will be most prominent on a small scale when strongly contrasting lithologies are juxtaposed (e.g., Hewitt, 1973; Ague and Rye, 1999).

## 5. CONCLUSIONS

This study reports, to our knowledge, the first direct measurements of $CO_2$-$H_2O$ interdiffusion rates at metamorphic temperatures and pressure. Diffusivities range from $\sim 1 \times 10^{-8}$ $m^2/s$ to $6 \times 10^{-8}$ $m^2/s$ for temperatures of 490 to 690°C, with a calculated activation energy for diffusion of 38 kJ/mol, which is virtually the same as that predicted by application of the Stokes-Einstein equation. This observation, combined with the fact that predicted and measured diffusivities are different only by a factor of ~2, supports application of Eqn. 3 to estimate diffusion coefficients for mixed fluids at elevated *P* and *T*.

Interdiffusion coefficients for $CO_2$ and $H_2O$ at the elevated *P* and *T* conditions of this study are within 2 orders of magnitude of values reported for the diffusion of heat ($\sim 1 \times 10^{-6}$ $m^2/s$) in rocks (e.g., Hoefer, 2002, and references therein). This confirms arguments made by many workers for rapid $CO_2$-$H_2O$ exchange during metamorphism, and for the need to incorporate diffusive fluxes into kinetic models of systems with heterogeneous fluid compositions, on both large and small scales.

*Acknowledgments*—We thank John Ferry, Christopher Breeding, and an anonymous reviewer for their insightful and constructive comments, as well as those of Eric Oelkers, *GCA* associate editor. Laura Klein, Jamie Prior, and Jonathan Price are also acknowledged for assisting at various stages of this project. This work was supported by the Office of Energy Research, U.S. Department of Energy, grant no. DE-FG02-94ER14432.

*Associate editor:* E. H. Oelkers

## REFERENCES

Ague J. J. (2000) Release of $CO_2$ from carbonate rocks during regional metamorphism of lithologically heterogeneous crust. *Geology* **28,** 1123–1126.

Ague J. J. (2002) Gradients in fluid composition across metacarbonate layers of the Wepawaug Schist, Connecticut, USA. *Contrib. Mineral. Petrol.* **143,** 38–55.

Ague J. J. and Rye D. M. (1999) Simple models of $CO_2$ release from metacarbonates with implications for interpretation of directions and magnitudes of fluid flow in the deep crust. *J. Petrol.* **40,** 1443–1462.

Aranovich L. Y. and Newton R. C. (1999) Experimental determination of $CO_2$-$H_2O$ activity-composition relations at 600-1000 degrees C and 6-14 kbar by reversed decarbonation and dehydration reactions. *Am. Mineral.* **84,** 1319–1332.

Berner R., Lasaga A., and Garrels R. (1983) The carbonate-silicate geochemical cycle and its effect on atmospheric carbon dioxide over the past 100 million years. *Am J. Sci.* **283,** 641–683.

Blencoe J. G., Seitz J. C., and Anovitz L. M. (1999) The $CO_2$-$H_2O$ system; II, calculated thermodynamic mixing properties for 400 degrees C, 0-400 MPa. *Geochim. Cosmochim. Acta* **63,** 2393–2408.

Cussler E. L. (1997) Diffusion: Mass Transfer in Fluid Systems. Cambridge University Press, Cambridge, UK.

Duan Z., Møller N., and Weare J. (1996) A general equation of state for supercritical fluid mixtures and molecular dynamics simulation of mixture PVTX properties. *Geochim. Cosmochim. Acta* **60,** 1209–1216.

Etheridge M., Wall V., Cox S., and Vernon R. (1984) High fluid pressures during regional metamorphism and deformation: implications for mass transport and deformation mechanisms. *J. Geophys. Res.* **89,** 4344–4358.

Frank M., Kuipers J., and van Swaaij W. (1996) Diffusion coefficients and viscosities of $CO_2$+$H_2O$, $CO_2$+$CH_3OH$, $NH_3$+$H_2O$, and $NH_3$+$CH_3OH$ liquid mixtures. *J. Chem. Eng. Data* **41,** 297–302.

Greenwood H. (1973) Thermodynamic properties of gaseous mixtures of $H_2O$ and $CO_2$ between 450° and 800°C and 0 to 500 bars. *Am J. Sci.* **273,** 561–571.

Hewitt D. A. (1973) The metamorphism of micaceous limestones from south-central Connecticut. *Am J. Sci.* **273-A,** 444–469.

Holness M. (1992) Equilibrium dihedral angles in the system quartz-$CO_2$-$H_2O$-NaCl at 800°C and 1-15 kbar: The effects of pressure and fluid composition on the permeability of quartzites. *Earth Planet. Sci. Lett.* **114,** 171–184.

Hoefer M. (2002) Heat-transfer in quartz, orthoclase, and sanidine at elevated temperature. *Phys. Chem. Miner.* **29,** 571–584.

Kerrick D. and Jacobs G. (1981) A modified Redllich-Kwong equation for $H_2O$, $CO_2$, and $H_2O$-$CO_2$ mixtures at elevated pressures and temperatures. *Am J. Sci.* **281,** 735–767.

Kerrick D. and Caldeira K. (1998) Metamorphic $CO_2$ degassing from orogenic belts. *Chem. Geol.* **145,** 213–232.

Labotka T. C., Nabelek P. I., and Papike J. J. (1988) Fluid infiltration through the Big Horse Limestone Member in the Notch Peak contact-metamorphic aureole, Utah. *Am. Mineral.* **73,** 1302–1324.

Lasaga A., Rye D., Lüttge A., and Bolton E. (2001) Calculation of fluid fluxes in Earth's crust. *Geochim. Cosmochim. Acta* **65,** 1161–1185.

Nigrini A. (1970) Diffusion in rock alteration systems: I. Prediction of limiting equivalent ionic conductances at elevated temperatures. *Am J. Sci.* **269,** 65–91.

Oelkers E. and Helgeson H. (1988) Calculation of the thermodynamic and transport properties of aqueous species at high pressures and temperatures: Aqueous tracer diffusion coefficients of ions to 1000°C and 5 kb. *Geochim. Cosmochim. Acta* **52,** 63–85.

Powell R. and Holland T. J. B. (1988) An internally consistent thermodynamic dataset with uncertainties and correlations: 3: Application methods, worked examples and a computer program. *J. Metamorph. Geol.* **6,** 173–204.

Seitz J. C. and Blencoe J. G. (1999) The $CO_2$-$H_2O$ system; I, experimental determination of volumetric properties at 400 degrees C, 10-100 MPa. *Geochim. Cosmochim. Acta* **63,** 1559–1569.

Skelton A., Bickle M., and Graham C. (1997) Fluid-flux and reaction rate from advective-diffusive carbonation of mafic sill margins in the Dalradian, southwest Scottish Highlands. *Earth Planet. Sci. Lett.* **146,** 527–539.

Tester J. W., Worley W. G., Robinson B. A., Grigsby C. O., and Freerer J. L. (1994) Correlating quartz dissolution kinetics in pure water from 25 to 625°C. *Geochim. Cosmochim. Acta* **58,** 2407–2420.

Walton M. (1960) Molecular diffusion rates in supercritical water vapor estimated from viscosity data. *Am J. Sci.* **258,** 385–401.

Walther J. and Orville P. (1982) Volatile production and transport in regional metamorphism. *Contrib. Mineral. Petrol.* **79,** 252–257.

Wark D. A. and Watson E. B (2002) Grain-scale channelization of pores due to gradients in temperature or composition of intergranular fluid or melt. *J. Geophys. Res.* **107,** paper number 2001JB000365.

Watson E. B. and Brenan J. (1987) Fluids in the lithosphere, 1. Experimentally-determined wetting characteristics of $CO_2$-$H_2O$ fluids and their implications for fluid transport, host-rock physical properties, and fluid inclusion formation. *Earth Planet. Sci. Lett.* **85,** 497–515.

Watson E. B. and Wark D. A. (1997) Diffusion of dissolved silica in $H_2O$ at 1.0 GPa, with implications for mass transport in the crust and upper mantle. *Contrib Mineral. Petrol.* **130,** 66–80.